

# Searching atomic spin contrast on nickel oxide (001) by force microscopy

M. Schmid, F. J. Giessibl,\* and J. Mannhart

Universität Augsburg, Institute of Physics, Electronic Correlations and Magnetism,  
Experimentalphysik VI, Universitätsstrasse 1, D-86135 Augsburg, Germany.

(Dated: June 28, 2018, submitted to Physical Review B)

The (001) surface of NiO, an antiferromagnet at room temperature, was investigated under ultra-high vacuum conditions with frequency modulation atomic force microscopy (FM-AFM). The antiferromagnetic coupling between ions leads to a spin superstructure on (001) surfaces. Exchange interaction between the probe of a force microscope and the NiO (001) surface should allow to image spin superstructures in real space. The surface was imaged with three different probing tips: nonmagnetic W tips, ferromagnetic Co tips and antiferromagnetic NiO tips - and atomic resolution was achieved with all three of them in various distance regimes and in several channels. Evidence for spin contrast was obtained in experiments that utilize NiO tips and oscillation amplitudes in the Å-regime, where optimal signal-to-noise ratio is expected. The spin contrast is weaker than expected and only visible in Fourier space images.

## INTRODUCTION

The electronic and mechanical properties of matter are dominated by the Coulomb interaction resulting from the charge of the electrons. In contrast, the magnetic interaction of the spin of the electrons plays a minor role. The dipole-dipole interaction of single electronic spins for typical interatomic distances is only on the order of a few  $\mu\text{eV}$  and electrostatic energies between two electrons are  $10^6$ -times larger. While the direct interaction energy between spins is small, the Pauli principle constrains the symmetry of wave functions of two-electron states depending on spin: the spatial part of a spin-singlet state must keep its sign with particle exchange, while a spin-triplet state flips the sign of the spatial part of the wave function with particle exchange. In  $\text{H}_2$ , the energetic difference between its two electrons occupying singlet- vs. triplet states (exchange interaction) amounts to several eV's [1]. Therefore, spin is important in solids, and it is important to establish tools that allow to analyze spin orientation on surfaces. For conductive samples, spin-polarized scanning tunneling microscopy [2] is a powerful tool to image the spin orientation of surface atoms within magnetic domains or even antiferromagnetic surfaces with atomic resolution [3]. Recently, the spin of a single magnetic ion has been measured by scanning tunneling spectroscopy [4]. However, the spin orientation is also of interest in insulating materials such as magnetic oxides. Insulators can be imaged by atomic force microscopy (AFM) [5], and magnetic force microscopy (MFM), a variation of AFM, allows magnetic imaging through the magnetic dipole interaction of magnetic domains in the probe tip and in the sample. Because of the weak dipole-dipole interaction, many spins comprising larger domains are necessary to measure magnetic dipole forces and the spatial resolution of magnetic force microscopy is limited to some 10 nm. In contrast, exchange interaction can lead to spin-dependent interaction energies of up to 100 meV, and atomic imaging of

exchange interactions on *ferromagnetic* samples by AFM has been proposed early after atomic resolution AFM became available [6]. For two reasons, antiferromagnetic samples are attractive to probe the possibility of exchange force measurements: a) they provide well-defined magnetic contrast over small lateral distances and b) the disturbing magnetic dipole interaction between a magnetic tip and an antiferromagnetic sample is weak and decays exponentially with distance. NiO (001) is a good choice for a test sample, because it is antiferromagnetic at room temperature and (001) surfaces with excellent flatness and cleanliness can be prepared relatively easily by cleavage in ultrahigh vacuum. Because of its magnetic properties, NiO is used as a pinning layer in spin valves and has been instrumental in the study of metal-insulator transitions [7]. Several groups have studied NiO (001) by atomic force microscopy and obtained atomic images of the surface [8, 9, 10, 11] and performed spectroscopy [12, 13, 14], but a clear-cut proof of the expected spin contrast is lacking. It has been proposed that spin contrast can only be observed at very small tip-sample distances [15], but this distance regime is difficult to reach with conventional AFM with soft cantilevers (spring constant  $k \approx 40 \text{ N/m}$ ) and large amplitudes ( $A \approx 10 \text{ nm}$ ). Also, conventional cantilevers are only available made from Si and magnetic layers need to be deposited on the cantilever which increases the tip radius. Here, we use stiff cantilevers with  $k \approx 4 \text{ kN/m}$  that can be operated at extremely small distances, even in the repulsive regime. Nevertheless, we did not see spin contrast even for very small distances using ferromagnetic tips. We argue below that the exchange interaction between ferromagnetic metal tips and NiO might be much smaller than exchange interaction in NiO bulk. We have therefore built force sensors that are equipped with NiO crystal tips and use them to image NiO(001). We use analysis in Fourier space to determine the extent of spin polarization and find some evidence in selected experiments using NiO tips.

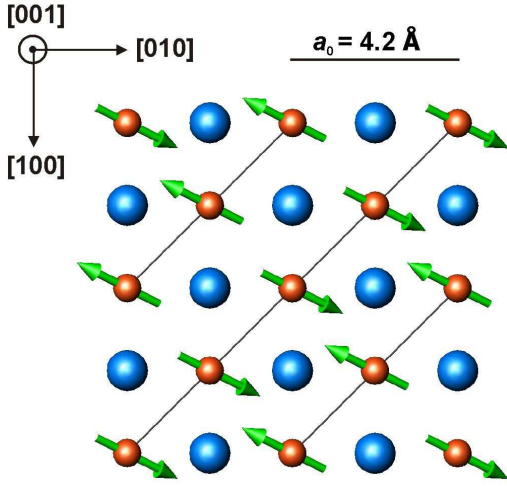


FIG. 1: (color online) NiO structure (spins located at the nickel sites): the top view onto the (001) surface shows ferromagnetic rows in  $\langle\bar{1}\bar{1}0\rangle$  direction which couple antiferromagnetically along the  $\langle110\rangle$  direction.

## EXPERIMENTAL

Nickel oxide crystallizes in the rock salt structure with a lattice constant of  $a_0 = 4.17\text{ \AA}$ . The spins are localized at the Ni sites and are pointing to one of the six possible  $\langle\bar{1}\bar{2}1\rangle$  directions [16]. NiO is an antiferromagnet with a Néel temperature well above room temperature at  $T_N = 525\text{ K}$ . Within the (111) planes, the spins couple ferromagnetically, the coupling between neighboring (111) planes is antiferromagnetic (see Fig. 1). The intersection of these planes with the (001) surface yields diagonals with parallel spin alignment, where neighboring lines have opposite spin directions.

The samples used in our experiments were single crystalline blocks of NiO (SurfaceNet, Rheine, Germany). They were cut to bars of about  $2 \times 4 \times 10\text{ mm}^3$  and mounted on a plate to allow sample transfer from ambient conditions to vacuum and *in situ* sample preparation. A gold layer of about 300 nm thickness was sputtered onto the samples to support the discharging of the surface right after cleavage. To obtain flat and clean surfaces, the crystals were cleaved *in-situ* with a UHV cleaving device [17]. All experiments were performed at room temperature at a pressure of  $\approx 8 \cdot 10^{-11}\text{ mbar}$ . Stable atomic imaging could be achieved for up to four days from the time the cleave was initiated, after that, contamination became visible clearly.

Several estimations of the expected exchange interaction between a magnetic tip and an antiferromagnetic sample surface have been published. First-principle calculations for two magnetic Fe(100) thin films with a distance in the range of the lattice constant yield  $E_{\text{ex}} \approx 10\text{ meV}$  and  $F_{\text{ex}} \approx 0.1\text{ nN}$  [18]. A modelling of

the NiO(001) surface interacting with a spin-polarized H atom (weakly reactive) and a spin-polarized Fe atom (strongly reactive) finds that the difference in force over opposite spin atoms should be detectable with the AFM for a tip-sample distance smaller than  $4\text{ \AA}$  or for imaging close to the repulsive regime [15]. However, at such short distances, the chemical bonding forces can become strong and it was speculated that ion instabilities may become apparent. Elongations of the tip and the sample atomic bonds are no longer negligible and atoms may even become displaced. They may lead to the loss of atomic resolution before the marginal tip-sample distance for detecting the exchange force is reached. Weakly reactive tips are less affected by these instabilities. For bulk NiO, Ködderitzsch *et al.* [19] have calculated that the AF<sub>2</sub> antiferromagnetic structure displayed in Fig. 1 has a bonding energy that is lower by 116 meV per Ni-O atom pair than a ferromagnetic spin arrangement. The Gibbs free energy of formation for NiO is 211 kJ/mol at room temperature [20], corresponding to 2.19 eV per Ni-O atom pair. Because every ion in NiO has six neighbors and every bond is shared by two ions, we estimate a bonding energy of 730 meV per bond. Therefore, the use of a NiO tip to probe NiO(001) promises to provide large spin-dependent contrast where the short-range bonding force varies by  $116\text{ meV}/730\text{ meV} = 16\%$ . The range of the exchange forces is expected to be similar to the range of chemical bonds with  $\lambda_{\text{ex}} \approx 0.1\text{ nm}$ .

Previous atomically resolved imaging experiments of NiO surfaces all have parameters in the following ranges: oscillation amplitudes of several nm and cantilevers with  $k \approx 40\text{ N/m}$  oscillating at frequencies of some hundreds of kHz [8, 9, 10, 11, 12, 13, 14]. Optimal signal-to-noise ratio is expected for oscillation amplitudes  $A \approx \lambda$  [21], where  $\lambda$  is the range of the interaction that is to be probed. Because of stability requirements,  $k \cdot A$  has to exceed a critical value [22] and a large stiffness is required for stable operation at small amplitudes. For this purpose, the self-sensing quartz cantilever qPlus [23], which is based on a commercial tuning fork and can be operated as is with oscillation amplitudes in the range of several Angstroms, was modified for operation at even smaller amplitudes. The stiffness of the prongs of the tuning fork is given by  $k = Ewt^3/4L^3$ , where  $L, t, w$  and  $E$  are the length, the thickness, the width and Youngs modulus of the prongs, respectively. The modification involved a shortening of the prongs by cutting them with a diamond wire saw, changing  $k$  from  $1800\text{ N/m}$  to  $\approx 4000\text{ N/m}$  and  $f_0$  from  $\approx 20\text{ kHz}$  to  $\approx 40\text{ kHz}$ . Stable oscillation at amplitudes of  $A \approx 1\text{ \AA}$  and below became possible with these ‘extra stiff’ qPlus sensors. Compared to the cantilevers of conventional AFM,  $k$  is increased by 100 allowing a decrease of  $A$  by a factor of 1/100. As a consequence, additional to the advantage of attenuated long-range background forces, qPlus extra stiff sensors promise to provide an increased frequency shift and thus higher resolution on

small scale.

The probe tips are important in AFM. Because of the large size and rigidity of our qPlus force sensors, a wide variety of tips can be mounted. Etched metal tips (e.g. W) as known from scanning tunneling microscopy are standard, but cobalt was chosen as a ferromagnetic tip material. Among the ferromagnetic elements it shows the weakest reactivity which facilitates stable imaging close to the sample surface. The etching was performed with a 50% solution of  $\text{HNO}_3$ . We also prepared antiferromagnetic tips made from NiO for reasons that are outlined below. NiO tips were prepared by cleaving larger crystals *ex situ* and searching for sharply pointed crystallites with sizes of roughly  $50\mu\text{m} \times 50\mu\text{m} \times 250\mu\text{m}$ . Annealing by electron bombardment in UHV is difficult for an insulator like NiO. Therefore, we attempted to clean the tips *in situ* by scratching along the (NiO) surface.

In typical AFM images of ionic crystals, only one type of ion appears as a protrusion, and the other type is imaged as a depression. It depends on the tip whether Ni or O ions are imaged as protrusions in AFM images of NiO (001). Momida et al. [24] argue that oxygen atoms appear as bright protrusions when using metal tips because metals react more strongly with oxygen than other metals. However, this issue and the identity of the tip atom and crystallographic environment constitute uncertainties in the image interpretation which will have to be discussed. Nevertheless, even if the oxygen atoms were imaged bright, contrast variations due to the exchange force are expected because a reduction of the symmetry at surface sites leads to a magnetic moment of the oxygen atoms, too. But this moment is estimated to be less than 10 % of the one over the nickel sites, so that the exchange effect is expected to be much less pronounced [25].

## RESULTS AND ANALYSIS

The NiO(001) surface was investigated with the improved cantilevers, which allow stable imaging at oscillation amplitudes as small as  $1\text{ \AA}$  and carry three different types of tips - nonmagnetic W tips, ferromagnetic Co tips and antiferromagnetic NiO tips (see Fig. 3a)). A large scale scan reveals step structures as shown in Fig. 2. The (001) surfaces are not ideal - a few screw dislocations are visible - but flat terraces with a width between  $0.05$  and  $0.5\mu\text{m}$  provide a good basis for atomic resolution.

Figure 3 shows that atomic contrast on flat and clean NiO(001) surfaces was obtained with all three kinds of tips (W, Co and NiO tips in b), c) and d), respectively). The exact parameters of the cantilevers are listed in table I.

The images were acquired at  $\Delta f = -20\text{ Hz}$ ,  $-23\text{ Hz}$  and  $-25\text{ Hz}$  with  $A \approx 1\text{ \AA}$ . Therefore, the normalized frequency shift  $\gamma = \Delta f k A^{3/2} / f_0$  was  $-2.4\text{ fN} \sqrt{\text{m}}$ ,  $-2.0\text{ fN} \sqrt{\text{m}}$  and  $-2.3\text{ fN} \sqrt{\text{m}}$ , respectively. Neighboring

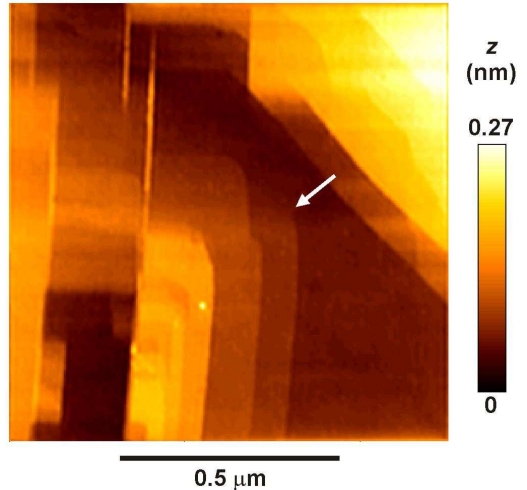


FIG. 2: (color online) Large scale step structure on NiO(001) revealed with FM-AFM equipped with a NiO tip ( $A \approx 2\text{ \AA}$ ,  $\Delta f = +15\text{ Hz}$ ). Between wide flat terraces few screw dislocations are visible, such as the one indicated by a white arrow.

	$f_0$ (Hz)	$k$ (N/m)
W tip	30675	3690
Co tip	40535	3540
NiO tip	43618	4020

TABLE I: Eigenfrequency and stiffness of the force sensors used in the experiments.

protrusions are spaced by roughly  $4\text{ \AA}$ , indicating that only one sort of atoms is imaged. A corrugation of around  $25\text{ pm}$  is observed in these topographical images. The chemical bonding forces responsible for the atomic resolution are assumed to be on the order of  $F_{\text{chem}} \approx 1\text{ nN}$  [26] – ten times larger than the expected exchange force ( $F_{\text{ex}} \approx 0.1\text{ nN}$ , see above). Contributions of the exchange interaction to the total tip-sample force are expected to cause about 10 percent of the total atomic corrugation. Because it is not clear whether Ni or O appears as a maximum and the exchange corrugation is expected to be maximal on top of Ni, we have to analyze both, maxima and minima, in line profiles.

A detailed investigation of the correlation between the imaging parameters and the corrugation (no images shown here) corroborates the intuitive expectations: Decreasing the oscillation amplitude leads to a much clearer resolution and, in addition, to an increased corrugation. Decreasing the set point of the frequency shift  $\Delta f$  causes a further approach to the sample surface. Hence, a greater influence of the short-range forces that lead to the atomic resolution is expected. Indeed the corrugation in associated height profiles of a corresponding series increases with increasing magnitude of the frequency shift setpoint. These measurements demonstrated that a

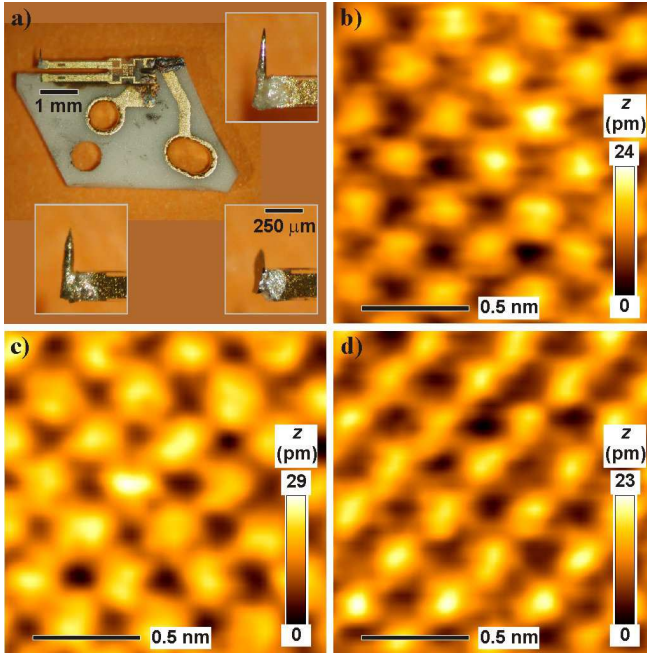


FIG. 3: (color online) qPlus sensors with tungsten (top), cobalt (bottom left) and nickel oxide (bottom right) tips as shown in a) allow FM-AFM with atomic resolution on NiO(001) surfaces; imaging parameters:  $A \approx 1 \text{ \AA}$  and b)  $\Delta f = -20 \text{ Hz}$  (W tip), c)  $\Delta f = -23 \text{ Hz}$  (Co tip), d)  $\Delta f = -25 \text{ Hz}$  (NiO tip).

small amplitude and a large frequency shift are key issues for good atomic resolution.

Therefore, we continuously decreased the frequency shift ( $\Delta f < 0$ ) while imaging at small amplitudes. Because of the large stiffness of the modified sensors and the careful choice of the tip material we were able to reach the repulsive regime, where  $\Delta f > 0$ . For the first time, atomic resolution of NiO(001) surfaces with a positive frequency shift, i.e. operation at a distance at or closer than the interatomic distance in bulk NiO, was achieved. It is important to note that we used  $\log |\Delta f|$  as a feedback signal, but we recorded  $\Delta f$  as well to confirm the sign of  $\Delta f$  (see Ref. [27] for more details). In Fig. 4a) a topographical image taken with a NiO tip at  $\Delta f = +66 \text{ Hz}$  and  $A \approx 1 \text{ \AA}$ , i.e.  $\gamma = +2.8 \text{ fN}\sqrt{\text{m}}$ , is presented. Simultaneously, the dissipation was recorded and the result is shown in Fig. 4b). The damping is determined from the driving amplitude that is necessary to keep the total energy of the cantilever constant. Variations in the dissipation therefore correspond to changes in the energy of the interactions [28]. Consequently, influences of the exchange force are expected to be detectable via the attributed changes in energy over adjacent atom sites in the dissipation channel, too. However, estimations yield that the ratio  $E_{\text{ex}}/E_{\text{chem}}$  is less favorable than the one of the forces  $F_{\text{ex}}/F_{\text{chem}} \approx 1/10$ .

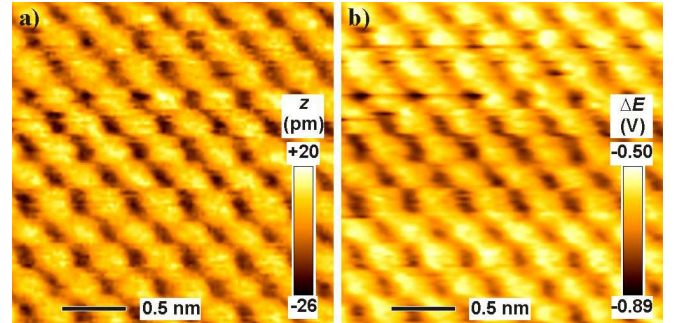


FIG. 4: (color online) Atomic resolution on NiO(001) obtained with FM-AFM in the repulsive mode. The images were taken with a NiO tip oscillating with  $A \approx 1 \text{ \AA}$  at  $\Delta f = +66 \text{ Hz}$ . a) is a topographical picture whereas b) presents the damping signals.

In total, a large variety of images was acquired showing atomic resolution with different tips in various distance regimes and several channels. As shown in Fig. 2, screw dislocations are present on this sample. We expect that screw dislocations alter the spin order, and even if spin alignment between tip and sample may be weak on one region, with all the surface regions that have been scanned there should be one region where spin alignment between tip and sample is sufficient to observe spin contrast. Possible spin order was searched by taking line profiles along the two directions of the diagonals and subsequent comparison. A more sensitive analysis method is offered by fast Fourier transformation (FFT) of the topographical images. The expected antiferromagnetic spin order of NiO (001) should reveal itself by a peak at half the spatial frequency of the fundamental lattice, thus additional Fourier peaks at  $(\frac{1}{2a_0}, \frac{1}{2a_0})$  or  $(\frac{1}{2a_0}, -\frac{1}{2a_0})$  should appear. The inset in Fig. 5 (a) presents the Fourier image of the main topographical image that was acquired with a NiO tip at  $\gamma = -9.0 \text{ fN}\sqrt{\text{m}}$  ( $\Delta f = -98 \text{ Hz}$  and  $A \approx 1 \text{ \AA}$ ). The expected additional peaks are not present in Figure . When integrating the intensity  $I$  of the FFT image over areas A, A', B, and B', the ratio  $(I_A + I_{A'} - I_B - I_{B'})/(I_A + I_{A'} + I_B + I_{B'})$  is a measure of spin polarization. In Figure 5 a) and the other images taken with W or Co tips, this ratio is approximately zero. In Figure 5 b), the spin polarization is  $\approx -10\%$ . Figure 5a) and 5b) were taken with a NiO tip, but at a slightly different lateral position and after a tip change that revealed itself by a glitched line and a contrast change. The main peaks at  $(\pm \frac{1}{a_0}, \pm \frac{1}{a_0})$  in the FFT image insets in Fig. 5 a) and b) have a height of 17 arbitrary units (a.u.), while the root-mean-square (rms) noise floor is at 3.0 a.u. and the areas B and B' are at 3.5 a.u. rms. In total, the superstructure has a corrugation of roughly  $\sqrt{3.5^2 - 3.0^2}/\sqrt{17^2 - 3.0^2} \times 25 \text{ pm} = 2.8 \text{ pm}$  – too small to be seen in the real space image but noticeable in the FFT image. Hence, the experimental spin

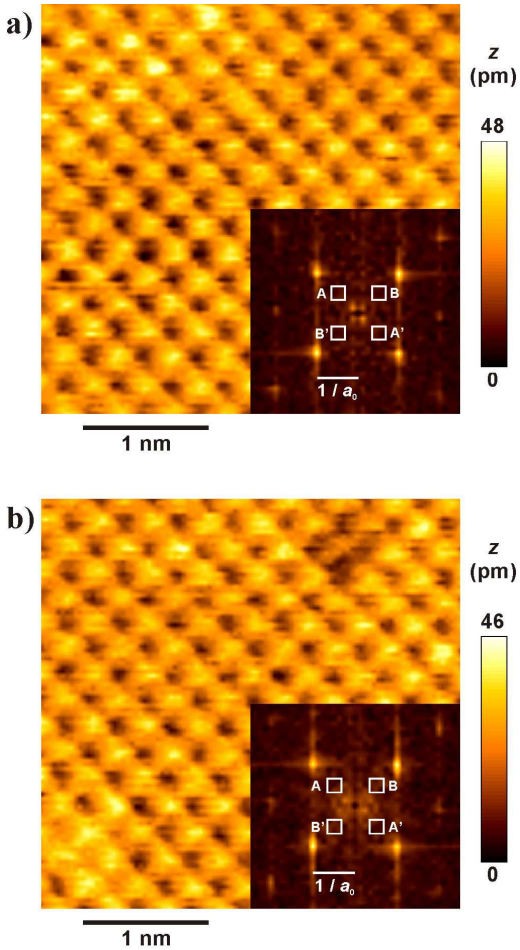


FIG. 5: (color online) a) FM-AFM image of a NiO(001) surface taken with a NiO tip at  $A \approx 1 \text{ \AA}$  and  $\Delta f = -98 \text{ Hz}$ . The presence of the two defects in the upper right and in the lower left corner shows that true atomic resolution is obtained, i.e. a single tip atom is responsible for imaging. The inset shows the central section of the Fourier transform of the topographical image. A peak at half the spatial frequency of one of the two base peaks would be visible if the contribution of the exchange interaction was larger than instrumental noise (see text). Here,  $(I_A + I_{A'} - I_B - I_{B'})/(I_A + I_{A'} + I_B + I_{B'}) \approx 0$ . b) Example where spin contrast appears to be present. The inset also shows the Fourier transformed image, where  $(I_A + I_{A'} - I_B - I_{B'})/(I_A + I_{A'} + I_B + I_{B'}) \approx -0.1$  (see text). The data presented in a) and b) was taken within the same measurement session, but a tip change indicated by a glitch and an overall contrast change had occurred between the images.

corrugation amplitude is 11 % of the fundamental corrugation, somewhat less than the 16 % estimate presented in the experimental section.

## DISCUSSION

The small extent of apparent spin contrast in most experimental images is puzzling. When assuming perfect spin alignment between tip and sample, the expected contribution of the exchange interaction is 16 times larger than the estimated instrumental noise level and 5 times larger than the observed best-case polarization. Calculations have shown that very small tip-sample distances are necessary to observe spin contrast even though tip ion instabilities may result at very small distance [29]. Here, we have been able to image in the repulsive regime with positive frequency shifts and generally at distances close to the bulk neighbor distance, where optimal spin contrast is expected [24]. While tips remained stable, we did not observe spin contrast in the expected magnitude. Stable imaging at a short tip-sample spacing with the ferromagnetic Co tips was possible because of Co's moderate reactivity with NiO. For revealing short-range magnetic forces, another parameter is highly important in addition to the tip-sample spacing, the relative orientation of the interacting spins. Ideally, tip and sample spin are aligned (anti-) parallel, but a misalignment of  $60^\circ$  is expected to yield half the maximal spin contrast (compare Fig. 6a)). Because there are six possible orientations for the spins in the NiO crystal and because we imaged large areas containing symmetry-breaking screw dislocations, for a given direction of the tip spin one domain has to exist where the deviation of the relative orientation of the spins is  $60^\circ$  at most. Considerations of the statistical partition of the spin alignments yield this maximum misalignment angle, too. When imaging NiO(001) the position on the surface and accordingly the investigated magnetic domain was changed multiple times. Therefore, we assume to find adequate spin alignment in several cases - at least for a limited time as we can not rule out spin flips of the tip but also within the sample during the scan.

A last consideration regards the tip material. The expected spin contrast originates in the exchange interaction, which is not due to a magnetic dipole-dipole interaction, but due to spin-controlled electrostatic interaction. Exchange interaction can only happen if a bonding orbital between tip and sample evolves, i.e. if an electronic state at a given energy has a large probability amplitude in both tip and sample atoms. The energy of the spin-polarized states located at the Ni sites of the NiO surface is about 0.7 Ryd below the Fermi level [19]. Approaching a metal tip - for example made from cobalt - to the NiO surface the Fermi levels will match. The spin-polarized states of the metal form a small band under the Fermi level with a bandwidth much smaller than the estimated 10 eV energy difference to the NiO surface. Consequently the formation of a molecular orbital that has a large amplitude on both tip and NiO sample appears to be un-

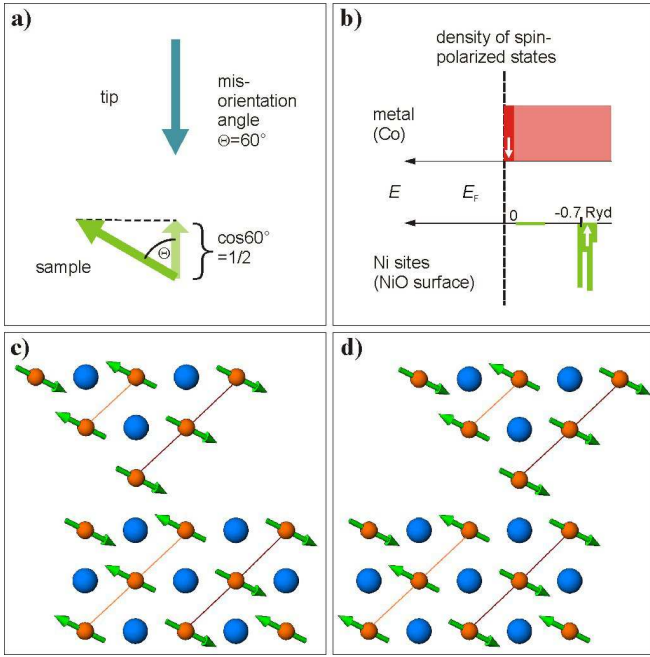


FIG. 6: (color online) a) Sketch illustrating the effect of a misalignment between tip and sample spin; b) comparison of density of spin-polarized states of the NiO surface and a metal tip revealing the improbability of an interaction; c) sketch of a Ni front atom located above a O sample atom such that spin order is preserved from tip to sample d) a Ni front atom also sits on top of a O sample atom, but the spin order is broken.

likely (compare Fig. 6b)). The result of this discussion is that ferromagnetic metal tips may not be the optimal choice for detecting exchange forces with a NiO sample. In spin-polarized tunneling, the physical mechanism behind spin contrast is different: the tunneling current is proportional to the spin-dependent density of states in tip and sample, and because electrons are tunneling from states close to the Fermi level in the tip (sample) into states close to the Fermi level in the sample (tip), the energetic equality is automatically fulfilled.

In order to obtain optimal tip-sample interactions we have chosen an approach that is conceptually very simple: we manufacture a tip of NiO and measure its interaction with a NiO surface. If the spin orientation in tip and sample was parallel, the spin orientation depicted in Fig. 6 c), where the spin order continues from tip to sample, is energetically lower than the one shown in Fig. 6 d), where the spin order is broken. It follows that the force in case 6 c) is larger than in 6 d). Spin contrast is expected to become visible no matter whether the tip atom is Ni or O, because the spin order could be continued in sequence in either case and spins between Ni ions couple through superexchange in NiO [30].

## SUMMARY AND OUTLOOK

In summary, we find evidence for spin contrast on NiO (001) in Fourier space images when using tips made from NiO and maximizing the sensitivity to short range forces by adapting a small amplitude scheme. Spin contrast was not detectable when using magnetized Co tips, and we have provided a qualitative explanation by arguing that the energy of the spin polarized states in Co tips and Ni ions on NiO does not match. This argument may explain why clear spin contrast has not been observed in very low noise experiments of other groups conducted at low temperatures. It is expected that the antiferromagnetic spin order of NiO (001) is fully developed at room temperature [19], but the tip atom of a sharp NiO crystallite may require much lower temperatures to develop spin order than the bulk. Therefore, we anticipate that the spin contrast signal will become stronger at low temperatures. Repeating this experiment at low temperatures with NiO tips will result in lower noise, such that spin order not only shows in Fourier images, but in real space images as well. Also, tip preparation can be improved. It would be beneficial to cleave the tips *in situ* in ultrahigh vacuum just as the sample. In this case, the tip would be definitely clean and uncontaminated, at least at the beginning of the experiment. The use of amplitudes in the Å- and sub-Å- regime was only possible by building force sensors with a stiffness on the order of 4 kN/m. Due to a careful choice of tip material, a small tip-sample distance could be realized without losing atomic contrast. These are essential requirements for detecting the extreme short-range exchange interaction between a magnetic tip and the antiferromagnetic sample surface. For the future, we plan to perform these measurements at low temperatures and to utilize advanced tip preparation methods such as *in situ* tip cleaving. The use of tips made from the same material as the sample has proven to be very successful. This concept may be transferable to other systems, expanding the conceptual beauty of break-junction experiments[31] to three dimensional imaging.

## ACKNOWLEDGMENTS

We thank T. Eguchi, Ch. Schiller and M. Breitschafft for helpful discussions and support. This work is supported by the Bundesministerium für Bildung und Forschung (project EKM13N6918) and by the European Science Foundation (THIOX).

\* Electronic address: franz.giessibl@physik.uni-augsburg.de

- [1] G. Baym, *Lectures on Quantum Mechanics* (W. A. Benjamin, Inc., New York, 1969).
- [2] M. Bode, Rep. Prog. Phys. **66**, 523 (2003).
- [3] S. Heinze, M. Bode, A. Kubetzka, O. Pietzsch, X. Nie, S. Blügel, and R. Wiesendanger, Science **288**, 1805 (2000).
- [4] A. J. Heinrich, J. A. Gupta, C. P. Lutz, and D. M. Eigler, Science **306**, 466 (2004).
- [5] G. Binnig, C. F. Quate, and Ch. Gerber, Phys. Rev. Lett. **56**, 930 (1986).
- [6] K. Nakamura, T. Oguchi, H. Hasegawa, K. Sueoka, K. Hayakawa, and K. Mukasa, Appl. Surf. Sci. **140**, 366 (1999).
- [7] M. Imada, A. Fujimori, and Y. Tokura, Rev. Mod. Phys. **70**, 4 (1309).
- [8] H. Hosoi, K. Sueoka, K. Hayakawa, and K. Mukasa, Appl. Surf. Sci. **157**, 218 (2000).
- [9] H. Hosoi, M. Kimura, K. Hayakawa, K. Sueoka, and K. Mukasa, Appl. Phys. A **72**, S23 (2001).
- [10] H. Hosoi, K. Sueoka, and K. Mukasa, Nanotechnology **15**, 505 (2004).
- [11] W. Allers, S. Langkat, and R. Wiesendanger, Appl. Phys. A **72**, S27 (2001).
- [12] H. Hölscher, S. M. Langkat, A. Schwarz, and R. Wiesendanger, Appl. Phys. Lett. **81**, 4428 (2002).
- [13] S. M. Langkat, H. Hölscher, A. Schwarz, and R. Wiesendanger, Surf. Sci. **527**, 12 (2003).
- [14] R. Hoffmann, M. A. Lantz, H. J. Hug, P. J. A. van Schendel, P. Kappenberger, S. Martin, A. Baratoff, and H.-J. Güntherodt, Phys. Rev. B **67**, 085402 (2003).
- [15] A. S. Foster and A. L. Shluger, Surf. Sci. **490**, 211 (2001).
- [16] F. U. Hillebrecht, H. Ohldag, N. B. Weber, C. Bethke, U. Mick, M. Weiss, and J. Bahrdt, Phys. Rev. Lett. **86**, 3419 (2001).
- [17] M. Schmid, A. Renner, and F. J. Giessibl, Rev. Sci. Instrum. **77**, 036101 (2006).
- [18] K. Nakamura, H. Hasegawa, T. Oguchi, K. Sueoka, K. Hayakawa, and K. Mukasa, Phys. Rev. B **56**, 3218 (1997).
- [19] D. Ködderitzsch, W. Hergert, W. M. Temmerman, Z. Szotek, A. Ernst, and H. Winter, Phys. Rev. B **66**, 064434 (2002).
- [20] D. R. Lide, ed., *CRC Handbook of Chemistry and Physics* (CRC Press, Boca Raton, 1996), 77th ed.
- [21] F. J. Giessibl, AIP Conference Proceedings **696**, 60 (2003).
- [22] F. J. Giessibl, Rev. Mod. Phys. **75**, 949 (2003).
- [23] F. J. Giessibl and H. Bielefeldt, Phys. Rev. B **61**, 9968 (2000).
- [24] H. Momida and T. Oguchi, Surf. Sci. **590**, 42 (2005).
- [25] H. Momida and T. Oguchi, J. Phys. Soc. Jpn. **72**, 588 (2003).
- [26] F. J. Giessibl, Materials Today **8(5)**, 32 (2005).
- [27] F. J. Giessibl and M. Reichling, Nanotechnology **16**, S118 (2005).
- [28] R. García and R. Pérez, Surf. Sci. Rep. **47**, 197 (2002).
- [29] A. S. Foster and A. L. Shluger, Surf. Sci. **490**, 211 (2001).
- [30] P. W. Anderson, Phys. Rev. **79**, 350 (1950).
- [31] N. Agrait, A. Yeyati, and J. van Ruitenbeek, Phys. Rep. **377**, 81 (2003).